CLAWAR 2013 343
Proceedings of the Sixteenth International Conference on
Climbing and Walking Robots, Sydney, Australia, 14 – 17 July 2013

CLIMBING ROBOT EQUIPPED WITH A POSTURAL ADJUSTMENT MECHANISM FOR CONICAL POLES*

YASUHIKO ISHIGURE†
Marutomi Seiko Co., Ltd., Kurachi Aza-Ikuda 3147-7
Seki, 501-3936, Japan

HARUHISA KAWASAKI,

TAICHI KATO, KATUYUKI HIRAI, NOBUYUKI IINUMA
Department of Human and Information Systems, Gifu University Yanagido 1-1,
Gifu, 501-1193, Japan

SATOSHI UEKI
Department of Mechanical Systems, Toyota National College of Technology,
Toyota, 471-8525, Japan

A climbing robot with a postural adjustment mechanism for conical poles is presented. The climbing method driven by servomotors with a warm-wheel reduction mechanism can rest on a tree by using its own weight without any energy expenditure. To realize both straight climbing and spiral climbing for conical poles, a postural adjustment mechanism is needed to move the steering mechanisms of the active wheels smoothly. We present the design of the robot's two-link arm mechanism with 1 DOF as the postural adjustment mechanism. It was demonstrated experimentally that the climbing robot, equipped with four active wheels, can straight climb and spiral climb conical poles by using the proposed postural adjustment mechanism.

1. Introduction

Robots that can climb poles are under development and are expected to be used in the inside/outside maintenance of buildings, observations of disaster scenes from a height, pruning trees, and more.

As an alternative, we developed and analyzed a climbing method [1, 2]. The climbing mechanism is equipped with a servomotor and a warm-wheel reduction mechanism which has non-back-drivability. It can stay on a tree using its own weight, since the center of its mass is located outside of the tree. A climbing

* This work was supported in part by the NEDO project (P03040) and the NARO Program for the Promotion of Basic and Applied Researches for Innovations in Bio-oriented Industry.

robot that uses its own weight, with one active wheel and two passive wheels, was described in 2010 [3, 4]. However, the climbing speed of the robot is low, since the robot can slip off when an active wheel slips. These robots can only climb straight up; they cannot climb in a spiral. Therefore, it is difficult to observe omnidirectionally and, for example, to prune trees after climbing up. Applications of climbing robots will be expanded if they can climb not only straight up but also spirally [2].

Most trees are conical thicker at the bottom and gradually becoming thinner with increasing height. This is called the stem taper in the logging/timber industry. When a climbing robot using its own weight climbs straight up a conical pole, the pole can get stuck in between the robot's wheels because the robot tilts downward as it climbs the conical pole. Moreover, it can be difficult to control the steering angle of the active wheels during the climb, even if the robot has not gotten stuck in the tree.

This paper proposes a postural adjustment mechanism to be used with a climbing robot that has four wheels. It consists of two 1-degree of freedom (DOF) two-link arm mechanisms, one located on the top side and the other underneath, to make the robot lightweight. The results of field experiments conducted in a forest are also presented.

2. Climbing robot using its own weight

2.1. *Mechanism of climbing robot using its own weight*

It is desirable that a climbing robot has more than two wheels, since it is quite possible for a wheel to slip out of place; more wheels will contribute to stable climbing. As shown in Figure 1, our climbing robot is equipped with four active wheels. Two wheels are located on top (numbers 1 and 2) and two wheels are located on the bottom (numbers 3 and 4). Each wheel is placed at the same angle $\pm \pi / 4$ rad relative to the $\boldsymbol{x}$-axis when viewed from the top of the cylinder. The active wheel is driven by a DC servomotor via a warm-wheel reduction mechanism. The warm-wheel reduction mechanism, which has non-back-drivability, allows the robot to be at rest without any energy expenditure when the input electric current for the servomotor is zero.

We ensured that the center of mass of the robot is located outside of the cylinder by placing the control system at the side of the down-side active wheels. Each of the four active wheels has a steering system to control the steering angle. The steering system is driven by a DC servomotor via a warm-wheel reduction mechanism.

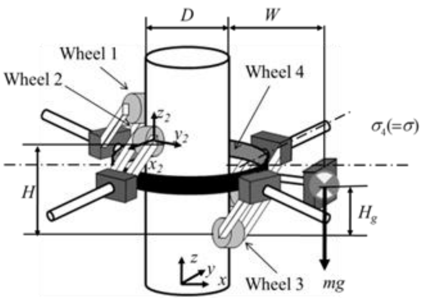

Fig. 1 Climbing robot equipped with four active wheel

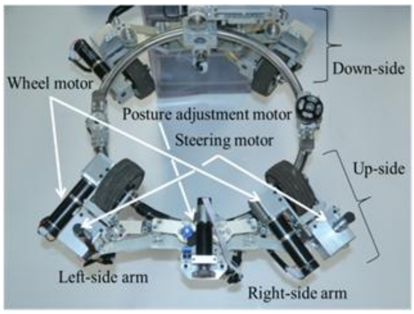

Fig. 2 Postural adjustment mechanism

3. Postural adjustment mechanism

3.1. *Mechanical structure*

A postural adjustment mechanism is necessary to help keep the weight of the robot down. As shown in Figure 2, we designed a postural adjustment mechanism that adjusts the posture of robot by moving two 1-DOF two-link arm mechanisms. The arms are located at the left side and right side such that the active wheel attached to the end link moves to the center of the pole. The arm mechanisms are placed at the top and bottom sides. The tilt of the robot is adjusted by controlling the servomotor, which moves the active wheels to the center of the pole and shortens the distance between the opposite wheels. The robot can rest without expending any energy, since the motor drives the arm joint via the warm-wheel reduction mechanism, which has non-back-drivability.

In this mechanism design using one degree of freedom, the active wheels move along the reference line (the dashed line in Figure 3), and it is desirable

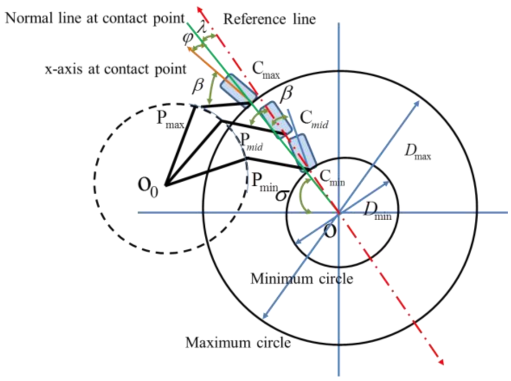

Fig. 3 Postural adjustment mechanism

that the posture of the wheel relative to the reference line at the contact point on the pole is not so large. In the figure, O is the origin of the base coordinate system fixed on the conical pole, O_0 is the origin of the arm base coordinate system, C_{max} is a contact point when the diameter of the pole is maximum (D_{max}), C_{min} is a contact point when the diameter of the pole is minimum (D_{min}), C_{mid} is a center point between C_{max} and C_{min}, P_i ($i=max,min,mid$) is a position vector of the end point of link 1 at C_i, and β is the mounting angle between the wheel and link 2.

3.2. *Design method*

The posture adjustment by the 1-DOF arm mechanism has a limit because the active wheel has three degrees of freedom in two-dimensional space. Hence, we defined a design guide as follows:

1. To maintain a wheel configuration that can resist an external force, a gap angle λ, which is defined as an angle between the reference line and the normal direction at the contact point, is less than about ± 5 deg as targeted.
2. To ensure a contact region of a wheel while avoiding uneven contact, a wheel posture φ, which is defined as an angle between the wheel travelling direction and the normal direction of the pole surface, is less than about ± 5 deg as targeted.
3. To reduce the mechanism's weight and to reduce the required torque at the arm joint, the total length of arms 1 and 2 is made as short as possible.
4. The 1st link is driven by the motor, and the 2nd link is driven by a four-linkage closed loop mechanism.

In order to satisfy these design guides, the length of the link mechanism was determined as follows:

a. On the contact points C_{max} and C_{min}, the wheel posture φ, the gap angle λ, and the origin position of the arm base coordinate system O_0 are given.
b. The mounting angle between the active wheel and link 2, β, is given, the end point of link 1 corresponding to C_i ($i=max,min,mid$), P_i, is calculated, and a relational expression of the length l_2 of link 2 is derived, which satisfies that an intersection of the perpendicular bisector between P_{max} and P_{mid} with the perpendicular bisector between P_{min} and P_{mid} coincides with the origin position of the arm base coordinate system O_0 .
c. The length l_1 of link 1 is calculated, and β is derived by seeking the minimum of the total length of the arm, $l = l_1 + l_2$.
d. The angle q_1 of link 1 which passes through P_i , and the angle q_2 of link 2

which passes through C_i are calculated for $i=max,min,mid$, and the length of the four-linkage mechanism is determined.

e. The wheel posture and the gap angle are derived with respect to the diameter of the pole. If these are within the acceptable ranges, then this process is finished. If it is not so, then the process is returned back to (a) after adjusting the position of the origin of the arm base coordinate system O_0.

3.3. *Numerical Calculation*

The relation between all link lengths and the mounting angle of the prototype climbing robot was derived using the Maple software program (Cybernet Systems Co., Ltd.).

Figure 4 shows the relation between the mounting angle and the total arm length and the relation between β and the absolute maximum $|\varphi|_{\max}$ and $|\lambda|_{\max}$ for φ and λ. It is hard to set both the total arm length and the maximum angle change best because the relation between them is conflicting relation. We therefore used $\beta=\pi/10$ rad, $l_1=98.4$ mm, and $l_2=86.9$ mm in the developed robot design. In this case, $|\varphi|_{\max}=0.058$ rad and $|\lambda|_{\max}=0.086$ rad.

The changes of the wheel posture φ and the gap angle λ with respect to the pole diameter are shown in Figure 5. Although the wheel posture varies according to the diameter of the pole, the design specification is almost satisfied.

This design method requires trial and error calculations. However, this is a useful design method for a 1-DOF mechanism that can generate three degrees of freedom planar motion of active wheels.

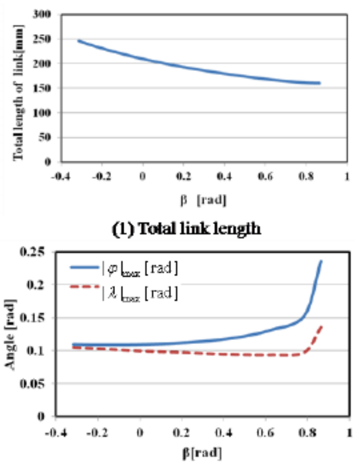

(1) Total link length

(2) Maximum posture variations of wheel

Fig. 4 Total link length and posture variations

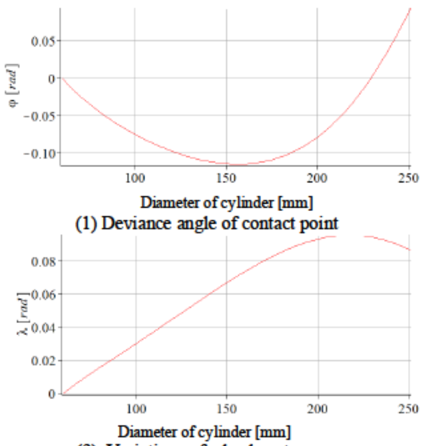

(1) Deviance angle of contact point

(2) Variations of wheel posture

Fig. 5 Variations of wheel posture and deviance angle of contact point

3.4. *Control method*

The tilt of the climbing robot is measured by the posture sensor. In order to match the central axis of the robot to that of the tree, one of the two arms (called the main arm) is implemented a posture PID control, and the other (called the slave arm) is implemented a joint-angle PID control in which the desired value is the arm joint angle of the main arm. That is, the posture PID control for the up-side arm is:

$$u_m(t) = k_{mP}(\theta_d - \theta(t)) - k_{mD}\dot{\theta}(t) + k_{mI}\int_0^t(\theta_d - \theta(t))dt \tag{8}$$

where $u(t)$ is the control input, k_{mP}, k_{mD}, k_{mI} are the proportional feedback gain, differential feedback gain, and integral feedback gain, respectively, and $\theta_d, \theta(t)$ are the desired posture angle and the measured posture angle, respectively. The actual desired posture angle is set to zero. The down-side arm is the slave arm, and the implemented joint-angle PID control law is expressed as follows:

$$u_s(t) = k_{sP}(q_m(t) - q_s(t)) - k_{sD}\dot{q}(t) + k_{sI}\int_{t_s}^t(q_m(t) - q_s(t))dt \tag{9}$$

where $q(t)$ is the angle of the 1st joint, subscript *m* is the main arm, and subscript *s* is the slave arm; the desired joint angle of the slave arm is set to be the joint angle of the main arm.

4. Experimental evaluation

4.1. *Developed climbing robot*

We developed a climbing robot to evaluate the effect of the posture adjustment mechanism. The robot can move up and down in both straight and spiral manners while the posture of the robot is regulated by the posture adjustment mechanism. There are four active wheels on the tip of the arm mechanisms which are driven by four 20-watt DC servomotors. Each DC motor is equipped with a rotary encoder and a planetary gear mechanism and coupled to a warm-wheel reduction mechanism. In addition, each active wheel has a steering mechanism driven by a 3-watt DC motor coupled to the warm-wheel reduction mechanism. Thus, the robot can move up and down spirally by the steering angle control.

A battery power supply and a control system are attached to the robot such that the center of the mass of the robot is located outside of the cylindrical pole. The control system consists of an FPGA-based control circuit and motor drive circuits. The robot is remote-controlled through a wireless LAN. The mass of the climbing robot, *m*, is 13.0 kg; the diameter of the active wheel is 0.075 m, and the outer dimensions of the robot are W = -0.005 m, H = 0.158 m.

4.2. *Experiment on a tree*

In generally, cedar and hinoki trees in the man-made forests in Japan have a tapering characteristic feature in which the diameter of the tree is reduced by approx. 0.01 m with each 1-m increase in height from the base of the tree [5]. To confirm the effect of the posture adjustment mechanism, we tested the climbing robot as shown in Figure 6 in an experimental forest. The tree was a hinoki with the breast-height diameter 0.155 m. The motion profile of the robot for the test was comprised of six motions: straight climbing upward for approx. 1.25 m, wheel steering with the steering angle 1.36 rad, spiral climbing for approx. 0.5 m, wheel steering with the steering angle -1.36 rad, straight moving down the tree, then stopping with posture adjustment. Figure 7 shows the experiment results for the position, velocity and posture of the robot.

Interval 1 is the straight climbing, intervals 2 and 4 are the wheel steering, interval 3 is the spiral climbing, and interval 5 is straight moving down. The velocity PI control was adopted for active wheels at moving up and down. The control gains of each wheel control system were the same. In Figure 7, the label "Desired" indicates the targeted value and "Wheel" shows the mean of the positions and velocities of the four active wheels, which were calculated from the rotation angle of the wheel motor and the diameter of the wheel. The Wheel position was almost equal to that of Desired, and the position error was approx. 0.1 m at the target climbing height 1.25 m, which occurred in association with sliding of the wheel. The Wheel velocity almost converged to the target velocity, 0.25 m/s. The posture of the robot changed not a little at the interval of straight climbing, due to the taper of the tree and the irregularity of the tree surface. However, the posture error was less than ± 0.02 rad during the steering interval and less than ± 0.04 rad during the spiral climbing; these values are within the tolerance level for wheel steering and pruning. These experimental results showed that the climbing robot with the posture adjustment mechanism can move up and down a tapered cylindrical column.


Fig. 6 Field test of the climbing robot

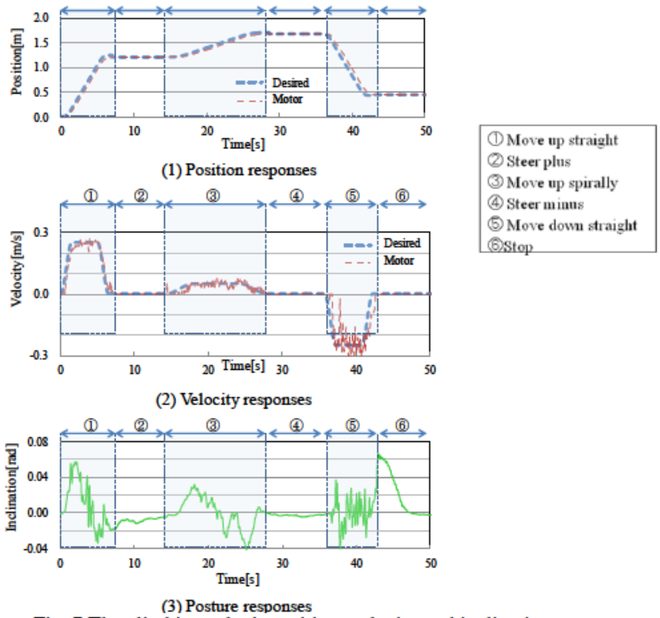

Fig. 7 The climbing robot's position, velocity and inclination responses to moving upward and downward (Left)

5. Conclusion

We have developed a novel climbing robot equipped with a posture adjustment mechanism consisting of two 1-DOF arms with joints located at the up-side and down-side. The robot can move straight up and down and spirally and can steer the active wheels in case of not only straight cylindrical poles but also conical poles. The robot can also remain stationary by using its own weight: no energy expenditure is needed to do so. The design method of the posture adjustment mechanism has also been presented. The robot's straight climbing velocity was 0.25 m/s, which is the fastest velocity among the existing climbing robots. We will evaluate the robot's ability to prune trees in the near feature.

References

1. H. Kawasaki, S. Murakami, H. Kachi, and S. Ueki, *Proc. of SICE Annual Conference 2008*. p. 160 (2008).
2. H. Kawasaki, S. Murakaki, K. Koganamaru, W. Chonnaparamuty, Y. Ishigure, and S. Ueki, *Proc. of CLAWAR 2010*. p. 455 (2010).
3. J. C. Fauroux and J. Morillon, *An International Journal*. **37:3**, p. 297 (2010)
4. A. Sadeghi, H. Moradi, and M. N. Ahmadabadi, *Robotica*. **30** (2011).
5. Website of Gifu Prefecture Reseach Institute for Forests, http://www.cc rd.pref.gifu.jp/forest/shiyou/hosori html (in Japanese).